

University of Dayton eCommons

Mechanical and Aerospace Engineering Faculty
Publications

Department of Mechanical and Aerospace
Engineering

8-2010

Pre-Swing Deficits in Forward Propulsion, Swing Initiation and Power Generation by Individual Muscles in Hemiparetic Walking

Carrie L. Peterson

University of Texas at Austin

Allison Kinney

University of Dayton, akinney2@udayton.edu


Steven A. Kautz

University of Florida

Richard R. Neptune

University of Texas at Austin

Follow this and additional works at: https://ecommons.udayton.edu/mee_fac_pub

 Part of the [Biomechanics Commons](#), [Biomedical Engineering and Bioengineering Commons](#), [Exercise Science Commons](#), [Mechanical Engineering Commons](#), and the [Other Kinesiology Commons](#)

eCommons Citation

Peterson, Carrie L.; Kinney, Allison; Kautz, Steven A.; and Neptune, Richard R., "Pre-Swing Deficits in Forward Propulsion, Swing Initiation and Power Generation by Individual Muscles in Hemiparetic Walking" (2010). *Mechanical and Aerospace Engineering Faculty Publications*. 29.

https://ecommons.udayton.edu/mee_fac_pub/29

This Article is brought to you for free and open access by the Department of Mechanical and Aerospace Engineering at eCommons. It has been accepted for inclusion in Mechanical and Aerospace Engineering Faculty Publications by an authorized administrator of eCommons. For more information, please contact frice1@udayton.edu, mschlangen1@udayton.edu.

Published in final edited form as:

J Biomech. 2010 August 26; 43(12): 2348–2355. doi:10.1016/j.jbiomech.2010.04.027.

PRE-SWING DEFICITS IN FORWARD PROPULSION, SWING INITIATION AND POWER GENERATION BY INDIVIDUAL MUSCLES DURING HEMIPARETIC WALKING

Carrie L. Peterson¹, Allison L. Hall¹, Steven A. Kautz^{2,3,4}, and Richard R. Neptune¹

¹Department of Mechanical Engineering, The University of Texas at Austin, TX

²Brain Rehabilitation Research Center, Malcom Randall VA Medical Center, Gainesville FL

³Department of Physical Therapy, University of Florida, Gainesville, FL

⁴Brooks Center for Rehabilitation Studies, University of Florida, Gainesville, FL

Abstract

Clinical studies of hemiparetic walking have shown pre-swing abnormalities in the paretic leg suggesting that paretic muscle contributions to important biomechanical walking subtasks are different than those of individuals without disability. Three-dimensional forward dynamic simulations of two representative hemiparetic subjects with different levels of walking function classified by self-selected walking speed (i.e., limited community = 0.4–0.8 m/s and community walkers = >0.8 m/s) and a speed-matched control were generated to quantify individual muscle contributions to forward propulsion, swing initiation and power generation during the pre-swing phase (i.e., double support phase preceding toe-off). Simulation analyses identified decreased paretic soleus and gastrocnemius contributions to forward propulsion and power generation as the primary impairment in the limited community walker compared to the control subject. The non-paretic leg did not compensate for decreased forward propulsion by paretic muscles during pre-swing in the limited community walker. Paretic muscles had the net effect to absorb energy from the paretic leg during pre-swing in the community walker suggesting that deficits in swing initiation are a primary impairment. Specifically, the paretic gastrocnemius and hip flexors (i.e., iliacus, psoas and sartorius) contributed less to swing initiation and the paretic soleus and gluteus medius absorbed more power from the paretic leg in the community walker compared to the control subject. Rehabilitation strategies aimed at diminishing these deficits have much potential to improve walking function in these hemiparetic subjects and those with similar deficits.

Keywords

post-stroke; modeling; simulation; three-dimensional; biomechanics

© 2010 Elsevier Ltd. All rights reserved.

Please address correspondence to: Richard R. Neptune, Ph.D., Department of Mechanical Engineering, University of Texas at Austin, 1 University Station C2200, Austin, TX 78712 USA, rneptune@mail.utexas.edu.

Publisher's Disclaimer: This is a PDF file of an unedited manuscript that has been accepted for publication. As a service to our customers we are providing this early version of the manuscript. The manuscript will undergo copyediting, typesetting, and review of the resulting proof before it is published in its final citable form. Please note that during the production process errors may be discovered which could affect the content, and all legal disclaimers that apply to the journal pertain.

Introduction

A central disability associated with post-stroke hemiparesis is impaired muscle excitation, which inhibits the generation of properly graded and timed muscle force (i.e., muscle coordination) necessary to perform important subtasks of walking. Of particular interest are those subtasks related to improving walking speed, which include forward propulsion (i.e., acceleration of the pelvis forward), swing initiation (i.e., power delivered to the swing leg) and power generation (i.e., production or absorption of mechanical energy). Recent studies have quantified muscle contributions to these subtasks in nondisabled subjects at self-selected and increasing steady-state speeds (Neptune et al. 2004; Neptune et al. 2008) and found that pre-swing (i.e., double support phase preceding toe-off) is a critical region of the gait cycle for muscles to accomplish these subtasks. Clinical studies of hemiparetic walking have shown pre-swing abnormalities in the paretic leg, including prolonged duration of the phase relative to the total gait cycle, reduced peak hip extension, and reduced hip and knee flexion velocities (De Quervain et al. 1996), suggesting that paretic muscle contributions to these subtasks are different than those of nondisabled walkers. Because walking speed depends largely on the person's ability to coordinate the paretic leg during pre-swing, understanding the relationships between impaired muscle coordination and walking speed in hemiparetic subjects during pre-swing would be extremely beneficial for designing effective locomotor interventions.

Due to dynamic coupling arising from the multiarticular nature of the musculoskeletal system (Zajac 1993), individual muscle function is difficult to assess via experimental techniques that use an inverse dynamics approach (Zajac et al. 2002). However, modeling and simulation techniques can quantify individual muscle contributions to body segment accelerations and power distribution. For example, simulation analyses of nondisabled walking have shown that soleus (SOL) and gastrocnemius (GAS) force output are both critical to power generation, while SOL is the primary contributor to forward propulsion and GAS is the primary contributor to swing initiation (Neptune et al. 2001; Zajac et al. 2003; Neptune et al. 2008). The hip flexors (e.g., iliacus, psoas (IL)) were also found to contribute to leg swing initiation (Neptune et al. 2004; Neptune et al. 2008).

Experimental studies of hemiparetic walking have reported several abnormalities during paretic pre-swing including deficits in electromyography (EMG) (Knutsson and Richards 1979; Lamontagne et al. 2002; Den Otter et al. 2007) and kinetic measures (Olney et al. 1994; Nadeau et al. 1999; Lamontagne et al. 2002; Chen et al. 2005) of the paretic plantar flexors. EMG recorded from paretic SOL and GAS show reduced and early excitation compared to nondisabled EMG patterns (Knutsson and Richards 1979; Den Otter et al. 2007). Chen et al. (2005) found differences in kinetic leg energy in hemiparetic subjects and speed-matched controls that suggest impaired paretic leg swing initiation. Other experimental studies have hypothesized that some hemiparetic subjects are able to compensate for paretic plantar flexor deficits and achieve faster walking speeds via the paretic hip flexors (Nadeau et al. 1999) and/or non-paretic leg force production (Bowden et al. 2006). For example, Nadeau et al. (1999) found weakness of the plantar flexors was correlated with gait speed limitations in a group of hemiparetic subjects, and some of these subjects who attained faster speeds produced an increased hip flexor moment. Bowden et al. (2006) reported that hemiparetic subjects with high and moderate severity relied heavily on the non-paretic leg to generate propulsion, which may do so during paretic pre-swing due to the changed orientation of the non-paretic leg. Specifically, in many hemiparetic subjects, the non-paretic foot is not as far forward at heel contact (relative to the pelvis) and flat for an extended time during paretic pre-swing compared to nondisabled walkers (Hsu et al. 2003; Chen et al. 2005; Balasubramanian et al. 2007). Because simulation analyses of nondisabled walking showed that the gluteus maximus (GMAX), vasti group (VAS) and hamstrings

(HAM) each contribute to forward propulsion and power generation during foot flat (Neptune et al. 2004), these non-paretic muscles may do so during paretic pre-swing.

The purpose of this study was to compare individual muscle contributions to forward propulsion, swing initiation and power generation of two representative hemiparetic subjects with different levels of walking function classified by self-selected speed (i.e., limited community = 0.4–0.8 m/s and community walkers = >0.8 m/s) (Perry et al. 1995) and speed and age-matched controls during pre-swing. We expected that: 1) GAS contribution to swing initiation, SOL contribution to forward propulsion and SOL and GAS power generation would be decreased; 2) swing initiation and power generation by the paretic hip flexors (e.g., IL) would be decreased for the limited community walker; and 3) forward propulsion and power generation provided by non-paretic GMAX, VAS and HAM during paretic leg pre-swing (i.e., early stance of the non-paretic leg) would be increased relative to controls. Because the stroke population is very heterogeneous, this study is a first step toward understanding the various impairments and compensatory mechanisms in post-stroke hemiparetic walking.

Methods

Experimental Data

Experimental data were collected from 51 hemiparetic subjects walking at self-selected speeds without use of an assistive device or ankle-foot orthosis and 21 nondisabled elderly subjects walking at self-selected speeds and speeds of 0.3, 0.6 and 0.9 m/s at the VA Brain Rehabilitation Research Center at the University of Florida as part of a larger study. A safety harness mounted to the ceiling that provided no body weight support protected the subjects in the event of loss of balance. All subjects signed informed consent and the Institutional Review Boards of the University of Florida and the University of Texas approved the protocol. Three-dimensional (3D) ground reaction forces (GRFs) and kinematics, and bilateral EMG from eight lower limb muscles (medial gastrocnemius, soleus, tibialis anterior, rectus femoris, vastus lateralis, biceps femoris, semimembranosus, and gluteus medius) were recorded at 2000 Hz, 100 Hz and 2000 Hz, respectively, during 30 s walking trials on a split-belt instrumented treadmill (Tecmachine) and were processed using Visual 3D (C-Motion, Inc.). Raw kinematic and GRF data were low-pass filtered using a fourth-order zero-lag Butterworth filter with cutoff frequencies of 6 Hz and 20 Hz, respectively. All data were time normalized to 100% of the paretic (ipsilateral, right for control) gait cycle and averaged across consecutive gait cycles within each subject at each speed. From this data set, walking trials of a representative subject from each functional group (limited community: male, left hemiparesis, single cerebrovascular infarction, age = 53 years, time post stroke = 2 years 1 month, self-selected treadmill speed = 0.45 m/s; community: male, left hemiparesis, single cerebrovascular infarction, age = 60 years, time post stroke = 8 years 5 months, self-selected treadmill speed = 0.9 m/s) and an age matched control subject (female, age = 59 years) walking at speeds of 0.6 and 1.0 m/s were selected for the simulation analysis. For these trials, the individual gait cycle with the minimum difference in joint angles and GRFs compared to the average data was used as tracking data (Fig. 1 and Fig. 2). For the hemiparetic subjects walking with self-selected overground and treadmill speeds within each functional group range, we selected the subject with the average percent of paretic propulsion value (Bowden et al. 2006) closest to the functional group average to represent each group.

Musculoskeletal Model

A previously developed 2D model and optimization framework (e.g., Neptune et al. 2008) were adapted to simulate 3D walking. The model was developed using SIMM

(MusculoGraphics, Inc.) with musculoskeletal geometry based on Delp et al. (1990) and consisted of rigid body segments representing the trunk, pelvis, and thigh, shank, talus, calcaneus and toes of each leg. The pelvis was allowed to translate and rotate with respect to the ground with six degrees-of-freedom (df) and the trunk was allowed to rotate relative to the pelvis with three df. Each hip joint was modeled with a spherical joint and each knee, ankle, subtalar, and metatarsal joint was modeled with a single df, yielding a total of 23 df in the model. The contact between the foot and ground was modeled with 31 independent visco-elastic elements on the bottom of each foot (Neptune et al. 2000). Passive torques representing the forces applied by ligaments, passive tissue and joint structures were applied at each joint (Anderson 1999). The dynamical equations-of-motion were derived using SD/FAST (PTC) and forward dynamics simulations were produced using Dynamics Pipeline (MusculoGraphics, Inc.).

The model had 43 Hill-type musculotendon actuators per leg. Muscle contraction dynamics were governed by Hill-type muscle properties (Zajac 1989) and muscle activation dynamics were modeled using a nonlinear first-order differential equation (Raasch et al. 1997) with activation and deactivation time constants derived from Winters and Stark (1988). Polynomial equations were used to estimate musculotendon lengths and moment arms (Menegaldo et al. 2004).

Dynamic Optimization

Forward dynamic simulations from paretic mid-stance to paretic toe-off (right leg for controls) were generated using dynamic optimization to test our hypotheses related to the pre-swing (double support) phase. A simulated annealing algorithm varied the muscle excitation patterns until differences between simulated and experimentally measured joint angles and GRFs were minimized (Goffe et al., 1994). Total muscle stress (muscle force/cross-sectional area of muscle) was also included in the cost function to minimize co-contraction while reproducing the experimental kinematics and GRFs equally well. Bimodal patterns (Eq. 1) were used to define the muscle excitations, $u(t)$, and were described by six optimization parameters including the onset, offset, and amplitude (A) of each mode i , at time t , for each muscle.

$$u(t) = \sum_{i=1}^2 \frac{A_i}{2} \left[1 - \cos \left(2\pi \cdot \frac{t - onset_i}{offset_i - onset_i} \right) \right] \quad (1)$$

Simulation Analyses

Previously described muscle-induced acceleration and segment power analyses (Fregly and Zajac 1996; Neptune et al. 2001) were used to quantify individual muscle contributions to forward propulsion (i.e., average horizontal acceleration of the pelvis), swing initiation (i.e., average mechanical power generated to the leg) and power generation (i.e., average musculotendon power) during paretic (right) leg pre-swing for each of the hemiparetic (control) simulations. The pre-swing double support phases corresponded to 19%, 16%, 14% and 13% of the gait cycle for the limited community, control at 0.6 m/s, community and control at 1.0 m/s simulations, respectively. After analysis, contributions by individual muscles were grouped according to their anatomical classification and how they contributed to the walking subtasks (Table 1).

Results

Simulations of limited community and community hemiparetic walkers and speed-matched controls were generated such that simulated GRFs and kinematics from mid-stance to toe-

off were near ± 2 standard deviations of the experimental data (Table 2). For clarification, we refer to the right and left leg of the control simulations (normalized to the right leg gait cycle) as the ipsilateral and contralateral leg, respectively, for comparison with the paretic and non-paretic legs. Paretic (ipsilateral) and non-paretic (contralateral) muscle excitation timings compared well with the experimental EMG and with data available in the literature (Den Otter et al. 2004; Den Otter et al. 2007).

Forward Propulsion

Paretic muscles contributed less to forward propulsion in the limited community hemiparetic walker compared to the ipsilateral leg of the speed-matched control (Fig. 3A, Net). For the limited community walker, forward propulsion by paretic SOL, GAS and GMED was decreased compared to the ipsilateral leg (Fig. 3A). The net effect of non-paretic muscles was to decelerate the pelvis during paretic pre-swing, in contrast with the net effect of the contralateral muscles of the control, which accelerated the pelvis forward (Fig. 3A). Non-paretic and contralateral VAS and RF in early stance contributed substantially to pelvis acceleration (Fig. 3A). Non-paretic and contralateral HAM contributed to pelvis deceleration, though much more in the limited community walker (Fig. 3A).

For the community hemiparetic walker, paretic SOL strongly accelerated the pelvis forward to provide more forward propulsion than ipsilateral SOL of the speed-matched control (Fig. 3B). Paretic and ipsilateral GAS provided forward propulsion secondary to SOL in the community walker and control (Fig. 3B). The total average pelvis acceleration and deceleration by paretic muscles was increased for the community walker compared to the ipsilateral leg due to increased acceleration by paretic GMED and increased deceleration by paretic AM (Fig. 3B). Non-paretic leg muscles contributed to forward propulsion in the community walker similar to the contralateral leg with HAM, VAS and RF being the primary contributors (Fig. 3B).

Swing Initiation

For the limited community walker, paretic muscles contributed more to swing initiation compared to the ipsilateral control leg (Fig. 4A, Net). Paretic and ipsilateral GAS was a primary contributor to swing initiation in both the limited community walker and control (Fig. 4A). Paretic IL contributed less to swing initiation and SAR contributed more to swing initiation in the limited community walker compared to the ipsilateral leg. Negative paretic swing initiation (i.e., power absorbed from the paretic leg by paretic muscles) was decreased relative to the ipsilateral leg due to reduced absorption by paretic SOL and GMED (Fig. 4A). Non-paretic leg muscles contributed to swing initiation in the limited community walker similar to the contralateral leg with HAM being the primary positive contributor and RF being the primary negative contributor (Fig. 4A).

For the community walker, paretic GAS, IL and SAR provided less and paretic AM provided more swing initiation compared to the ipsilateral leg (Fig. 4B). The total average power absorbed by paretic leg muscles of the community walker was increased relative to the ipsilateral leg as paretic SOL and GMED absorbed more power from the paretic leg, such that the net effect of paretic muscles was to absorb power from the paretic leg during pre-swing (Fig. 4B, Net). Similar to the control, non-paretic HAM and RF were primary contributors to swing initiation in the community walker (Fig. 4B).

Power Generation

For the limited community walker, paretic muscles generated less power compared to the ipsilateral control leg (Fig. 5A: Total), specifically with the paretic GAS generating much less power (Fig. 5A). Paretic SOL and GMED absorbed power in the limited community

walker, while ipsilateral SOL and GMED generated power in the control (Fig. 5A). Power generated by non-paretic and contralateral muscles was similar for the limited community walker and control (Fig. 5A: Total).

The community walker also generated less power with paretic leg muscles compared to the control (Fig. 5B: Total) with the primary deficits in power generation by the paretic SOL and GAS (Fig. 5B). Power absorption by paretic muscles was increased in the community walker compared to the control (Fig. 5B: Total) as the paretic GMED and AM absorbed power in addition to the paretic VAS (Fig. 5B). Power generated by non-paretic and contralateral muscles was similar for the community walker and control (Fig. 5B: Total).

Discussion

The purpose of this study was to use 3D muscle-driven forward dynamics simulations to compare individual muscle contributions to forward propulsion, swing initiation and power generation of two hemiparetic subjects with different levels of walking function classified by self-selected walking speed with those from nondisabled age and speed-matched controls during pre-swing. The simulation analyses identified decreased forward propulsion and power generation by paretic muscles in the limited community hemiparetic walker compared to the control. For the community hemiparetic walker, paretic leg muscles contributed less to swing initiation and generated less power compared to the control.

Limited Community Hemiparetic Walker: Forward propulsion is primary impairment

We expected that the SOL contribution to forward propulsion and power generation would be decreased in the paretic leg relative to the controls. Indeed for the limited community hemiparetic walker, paretic SOL contributed less to forward propulsion compared to the speed-matched control (Fig. 3A). In addition to SOL, the paretic GAS and GMED contributed less to forward propulsion (Fig. 3A) and paretic SOL, GAS and GMED each generated less power (Fig. 5A). Because SOL is the primary contributor to forward propulsion and GAS also accelerates the trunk during pre-swing in nondisabled walking (Neptune et al. 2000;McGowan et al. 2008), these results suggest that the decreased paretic SOL and GAS contribution to forward propulsion is likely an important factor limiting walking speed for the limited community walker, consistent with previous experimental studies of hemiparetic walking (Nadeau et al. 1999;Jonkers et al. 2009).

We also expected that non-paretic GMAX, VAS and HAM contributions to forward propulsion and power generation during the paretic leg pre-swing would be increased relative to controls. For the limited community walker, the net non-paretic leg contribution to forward propulsion was negative as non-paretic HAM contributed more to negative forward propulsion compared to the contralateral control leg. Thus, the non-paretic leg did not compensate for decreased forward propulsion by paretic muscles during pre-swing. Because the net forward propulsion by both legs (Fig. 3A, sum of paretic and non-paretic Net) was near zero (-0.462 m/s^2) for the limited community walker during paretic pre-swing, forward propulsion must be generated during another phase of the gait cycle (e.g., non-paretic pre-swing) to maintain walking speed (Morita et al. 1995).

We expected that GAS and hip flexor contributions to swing initiation and power generation would be decreased in the paretic leg of the limited community walker relative to the control. In contrast to our expectation, paretic muscles contributed to swing initiation similar to the ipsilateral leg (Fig. 4A, Total), including paretic GAS and the hip flexors (i.e., sum of IL and SAR) (Fig. 4A). Negative contributions to swing initiation by paretic muscles (Fig. 4A, primarily paretic SOL and GMED) were decreased relative to the ipsilateral leg. In the

control subject walking at 0.6 m/s, ipsilateral SOL and GMED absorbed much energy from the ipsilateral leg to control the leg during slow walking.

Community Hemiparetic Walker: Swing initiation is primary impairment

Paretic muscles had the net effect to absorb energy from the paretic leg during pre-swing suggesting that paretic swing initiation is impaired in the community hemiparetic walker. Paretic GAS, IL and SAR contributed less to paretic swing initiation, paretic AM contributed more, and paretic SOL and GMED absorbed much more power from the paretic leg in the community walker relative to the ipsilateral leg (Fig. 4B). The decreased paretic GAS and hip flexor contributions to swing initiation and increased paretic AM and GMED contributions to positive and negative swing initiation, respectively, is consistent with an experimental study that found impaired swing initiation of the paretic leg that was related to compensatory strategies (e.g., pelvic hiking) during swing among hemiparetic subjects and speed-matched controls (Chen et al. 2005). Also, the mechanism of SOL to decelerate the leg during pre-swing as it transfers energy from the leg to the trunk was observed in a previous 2D simulation of nondisabled walking (Neptune et al. 2001). This mechanism was found in the present 3D simulation of the community walker by paretic SOL to strongly decelerate the paretic leg (i.e., SOL transferred energy from the leg to the pelvis), and also by GMED (Fig. 4B).

The community walker was not limited by the ability to generate forward propulsion with the paretic leg, consistent with adequate paretic propulsive impulses generated by low severity hemiparetic subjects reported previously (Bowden et al. 2006). The community walker relied heavily on the paretic SOL to provide forward propulsion as it contributed more to forward propulsion compared to the control (Fig. 1B). Paretic muscles contributed more to positive and negative forward propulsion (Fig. 3B, Total) for the community walker compared to the control, primarily due to increased contributions by paretic GMED and AM (Fig. 3B). Paretic GAS contributed to forward propulsion in the community walker similar to ipsilateral GAS in the control (Fig. 3B), though its contribution was less than SOL, which is consistent with previous studies of nondisabled walking (Neptune et al. 2001; McGowan et al. 2008).

Limitations

We analyzed treadmill walking which induces subtle differences compared to overground walking. However, the contributions of individual muscles to the subtasks are unlikely to be different overground because they are completely determined by the state (i.e., positions and velocities of the body segments) of the system (Zajac et al. 2003). A potential limitation with this study was the use model parameters based on nondisabled subjects to simulate the hemiparetic subjects. However, because muscle force is scaled by the excitation magnitude, which is determined by the optimization algorithm to emulate the experimental data, the simulated forces used to assess muscle function are relatively insensitive to model parameters. Furthermore, we constrained the muscle excitation timing in the optimization to match closely with measured EMG timing. Because muscle coordination deficits of hemiparetic subjects result in various patterns of walking dysfunction, it is not known how well the results from the two representative hemiparetic subjects generalize to other hemiparetic subjects of their functional walking status. We expect that others walking with similar kinematics and kinetics would exhibit similar deficits during paretic pre-swing as observed in the current study.

Conclusions

We found deficits in paretic muscle contributions to forward propulsion and swing initiation during paretic pre-swing compared to the speed-matched control in the limited community

and community hemiparetic subjects, respectively. Rehabilitation strategies aimed at diminishing these deficits have much potential to improve walking function in these hemiparetic subjects and those with similar deficits. Future work should focus on developing simulations of more hemiparetic subjects including other regions of the gait cycle to provide additional insight into impairments in muscle function in the post-stroke hemiparetic population.

Acknowledgments

The authors would like to thank Erin Carr, Dr. Mark Bowden, Bhavana Raja, Cameron Nott, Dr. Chitra Balasubramanian and Ryan Knight for help with the data collection and processing. This work was funded by NIH grant RO1 HD46820, the Rehabilitation Research & Development Service of the VA and a NSF Graduate Research Fellowship.

References

- Anderson, FC. A dynamic optimization solution for a complete cycle of normal gait. Austin, TX: The University of Texas at Austin; 1999.
- Balasubramanian CK, Bowden MG, Neptune RR, Kautz SA. Relationship between step length asymmetry and walking performance in subjects with chronic hemiparesis. *Arch Phys Med Rehabil.* 2007; 88(1):43–49. [PubMed: 17207674]
- Bowden MG, Balasubramanian CK, Neptune RR, Kautz SA. Anterior-posterior ground reaction forces as a measure of paretic leg contribution in hemiparetic walking. *Stroke.* 2006; 37(3):872–876. [PubMed: 16456121]
- Chen G, Patten C, Kothari DH, Zajac FE. Gait differences between individuals with post-stroke hemiparesis and non-disabled controls at matched speeds. *Gait Posture.* 2005; 22(1):51–56. [PubMed: 15996592]
- De Quervain IA, Simon SR, Leurgans S, Pease WS, McAllister D. Gait pattern in the early recovery period after stroke. *J Bone Joint Surg Am.* 1996; 78(10):1506–1514. [PubMed: 8876578]
- Delp SL, Loan JP, Hoy MG, Zajac FE, Topp EL, Rosen JM. An interactive graphics-based model of the lower extremity to study orthopaedic surgical procedures. *IEEE Trans Biomed Eng.* 1990; 37(8):757–767. [PubMed: 2210784]
- Den Otter AR, Geurts AC, Mulder T, Duysens J. Speed related changes in muscle activity from normal to very slow walking speeds. *Gait Posture.* 2004; 19(3):270–278. [PubMed: 15125916]
- Den Otter AR, Geurts AC, Mulder T, Duysens J. Abnormalities in the temporal patterning of lower extremity muscle activity in hemiparetic gait. *Gait Posture.* 2007; 25(3):342–352. [PubMed: 16750632]
- Fregly BJ, Zajac FE. A state-space analysis of mechanical energy generation, absorption, and transfer during pedaling. *J Biomech.* 1996; 29(1):81–90. [PubMed: 8839020]
- Goffe WL, Ferrier GD, Rogers J. Global optimization of statistical functions with simulated annealing. *Journal of Econometrics.* 1994; 60:65–99.
- Hsu AL, Tang PF, Jan MH. Analysis of impairments influencing gait velocity and asymmetry of hemiplegic patients after mild to moderate stroke. *Arch Phys Med Rehabil.* 2003; 84(8):1185–1193. [PubMed: 12917858]
- Jonkers I, Delp S, Patten C. Capacity to increase walking speed is limited by impaired hip and ankle power generation in lower functioning persons post-stroke. *Gait Posture.* 2009; 29(1):129–137. [PubMed: 18789692]
- Knutsson E, Richards C. Different types of disturbed motor control in gait of hemiparetic patients. *Brain.* 1979; 102(2):405–430. [PubMed: 455047]
- Lamontagne A, Malouin F, Richards CL, Dumas F. Mechanisms of disturbed motor control in ankle weakness during gait after stroke. *Gait Posture.* 2002; 15(3):244–255. [PubMed: 11983499]
- McGowan CP, Neptune RR, Kram R. Independent effects of weight and mass on plantar flexor activity during walking: implications for their contributions to body support and forward propulsion. *J Appl Physiol.* 2008; 105(2):486–494. [PubMed: 18556431]

- Menegaldo LL, de Toledo Fleury A, Weber HI. Moment arms and musculotendon lengths estimation for a three-dimensional lower-limb model. *J Biomech.* 2004; 37(9):1447–1453. [PubMed: 15275854]
- Morita S, Yamamoto H, Furuya K. Gait analysis of hemiplegic patients by measurement of ground reaction force. *Scand J Rehabil Med.* 1995; 27(1):37–42. [PubMed: 7792548]
- Nadeau S, Gravel D, Arseneault AB, Bourbonnais D. Plantarflexor weakness as a limiting factor of gait speed in stroke subjects and the compensating role of hip flexors. *Clin Biomech (Bristol, Avon).* 1999; 14(2):125–135.
- Neptune RR, Kautz SA, Zajac FE. Contributions of the individual ankle plantar flexors to support, forward progression and swing initiation during walking. *J Biomech.* 2001; 34(11):1387–1398. [PubMed: 11672713]
- Neptune RR, Sasaki K, Kautz SA. The effect of walking speed on muscle function and mechanical energetics. *Gait Posture.* 2008; 28(1):135–143. [PubMed: 18158246]
- Neptune RR, Wright IC, Van Den Bogert AJ. A Method for Numerical Simulation of Single Limb Ground Contact Events: Application to Heel-Toe Running. *Comput Methods Biomech Biomed Engin.* 2000; 3(4):321–334. [PubMed: 11264857]
- Neptune RR, Zajac FE, Kautz SA. Muscle force redistributes segmental power for body progression during walking. *Gait Posture.* 2004; 19(2):194–205. [PubMed: 15013508]
- Olney SJ, Griffin MP, McBride ID. Temporal, kinematic, and kinetic variables related to gait speed in subjects with hemiplegia: a regression approach. *Phys Ther.* 1994; 74(9):872–885. [PubMed: 8066114]
- Perry J, Garrett M, Gronley JK, Mulroy SJ. Classification of walking handicap in the stroke population. *Stroke.* 1995; 26(6):982–989. [PubMed: 7762050]
- Raasch CC, Zajac FE, Ma B, Levine WS. Muscle coordination of maximum-speed pedaling. *J Biomech.* 1997; 30(6):595–602. [PubMed: 9165393]
- Winters JM, Stark L. Estimated mechanical properties of synergistic muscles involved in movements of a variety of human joints. *J Biomech.* 1988; 21(12):1027–1041. [PubMed: 2577949]
- Zajac FE. Muscle and tendon: properties, models, scaling, and application to biomechanics and motor control. *Crit Rev Biomed Eng.* 1989; 17(4):359–411. [PubMed: 2676342]
- Zajac FE. Muscle coordination of movement: a perspective. *J Biomech.* 1993; 26 Suppl. 1:109–124. [PubMed: 8505346]
- Zajac FE, Neptune RR, Kautz SA. Biomechanics and muscle coordination of human walking. Part I: introduction to concepts, power transfer, dynamics and simulations. *Gait Posture.* 2002; 16(3): 215–232. [PubMed: 12443946]
- Zajac FE, Neptune RR, Kautz SA. Biomechanics and muscle coordination of human walking: part II: lessons from dynamical simulations and clinical implications. *Gait Posture.* 2003; 17(1):1–17. [PubMed: 12535721]

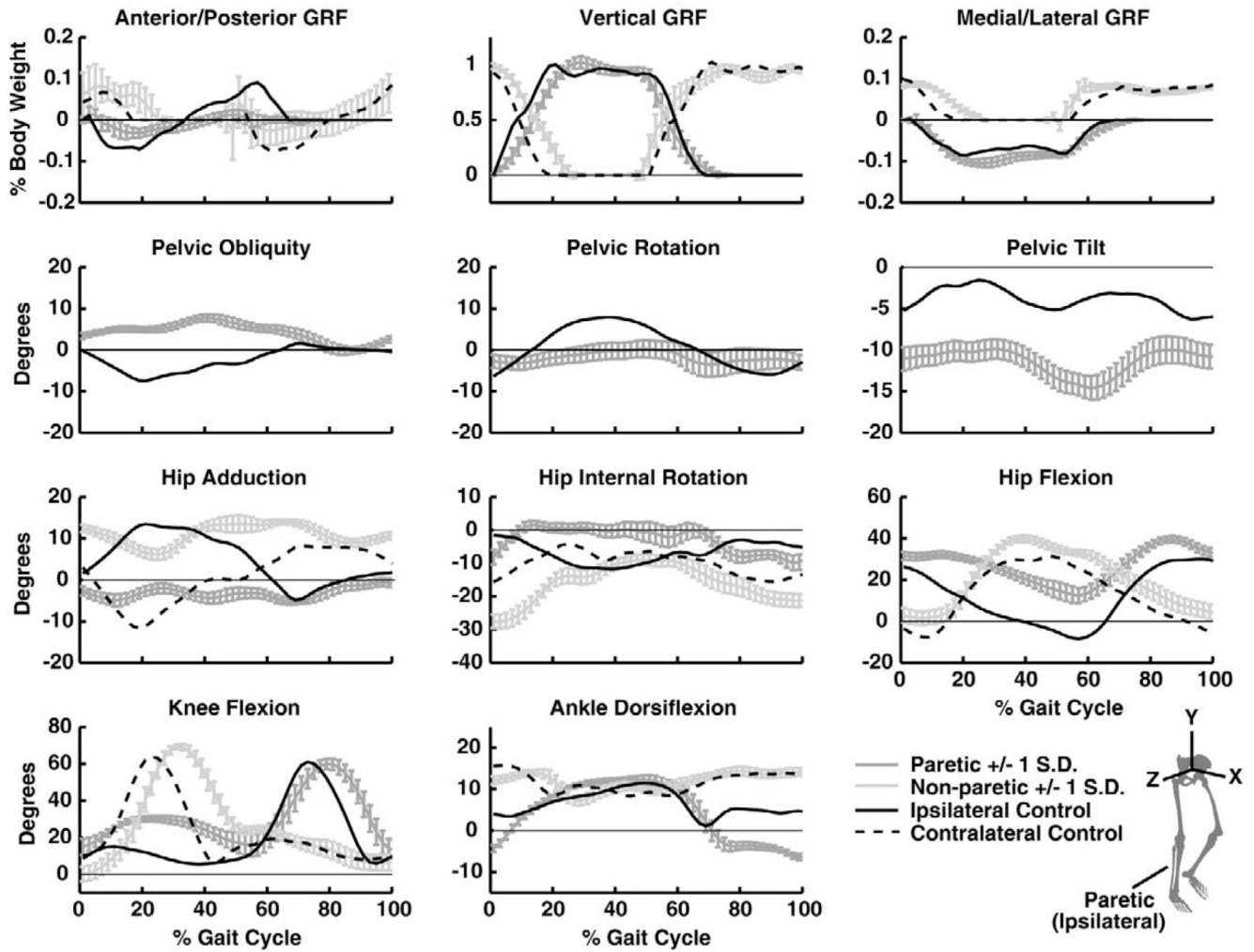


Fig. 1. Experimental data of the gait cycle with minimum difference in joint angles and ground reaction forces (GRFs) compared to the subject's average for the limited community walker at self-selected speed (with ± 1 standard deviation (S.D.) of the 30 s walking trial) and the control walking at 0.6 m/s. Data are normalized to the paretic (ipsilateral) gait cycle. Joint angle subtitles correspond to positive directions. Positive pelvic obliquity, rotation and tilt correspond to positive rotations about the X, Y and Z pelvis segment axes, respectively (see bottom right).

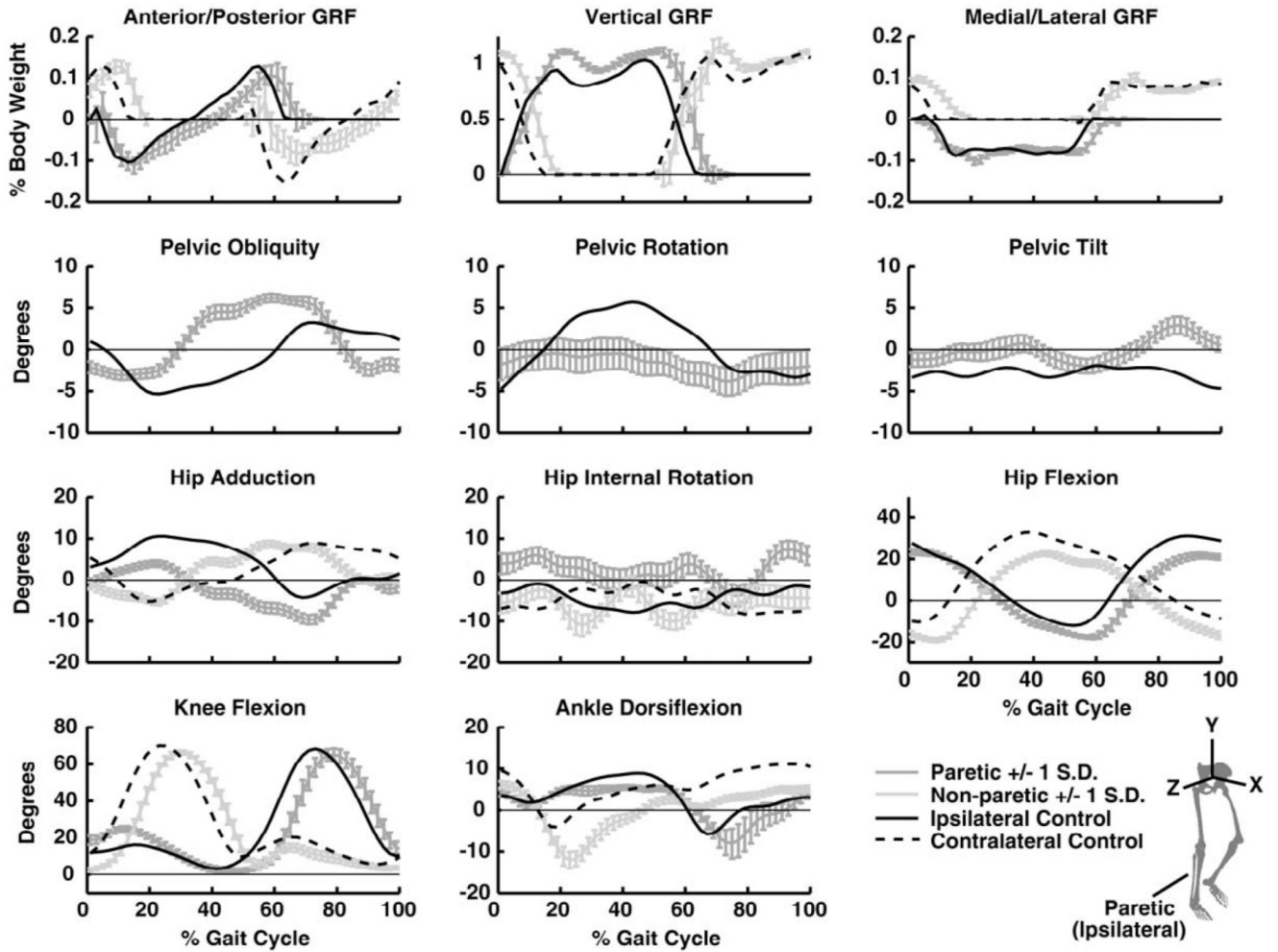


Fig. 2. Experimental data of the gait cycle with minimum difference in joint angles and ground reaction forces (GRFs) compared to the subject's average for the community walker at self-selected speed (with ± 1 standard deviation (S.D.) of the 30 s walking trial) and the control walking at 1.0 m/s. Data are normalized to the paretic (ipsilateral) gait cycle. Joint angle subtitles correspond to positive directions. Positive pelvic obliquity, rotation and tilt correspond to positive rotations about the X, Y and Z pelvis segment axes, respectively (see bottom right).

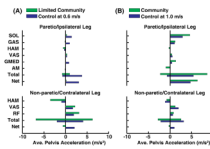


Fig. 3. Primary muscle contributors to forward propulsion (i.e., average horizontal pelvis acceleration) and the total average pelvis acceleration and deceleration (Total) and net by all paretic (ipsilateral for control) and non-paretic (contralateral for control) muscles during pre-swing. (A) For the limited community walker, forward propulsion provided by paretic and non-paretic muscles were decreased and increased, respectively, compared to the speed-matched control. (B) Forward propulsion provided by paretic muscles (i.e., SOL and GMED) was increased in the community walker relative to the speed-matched control.

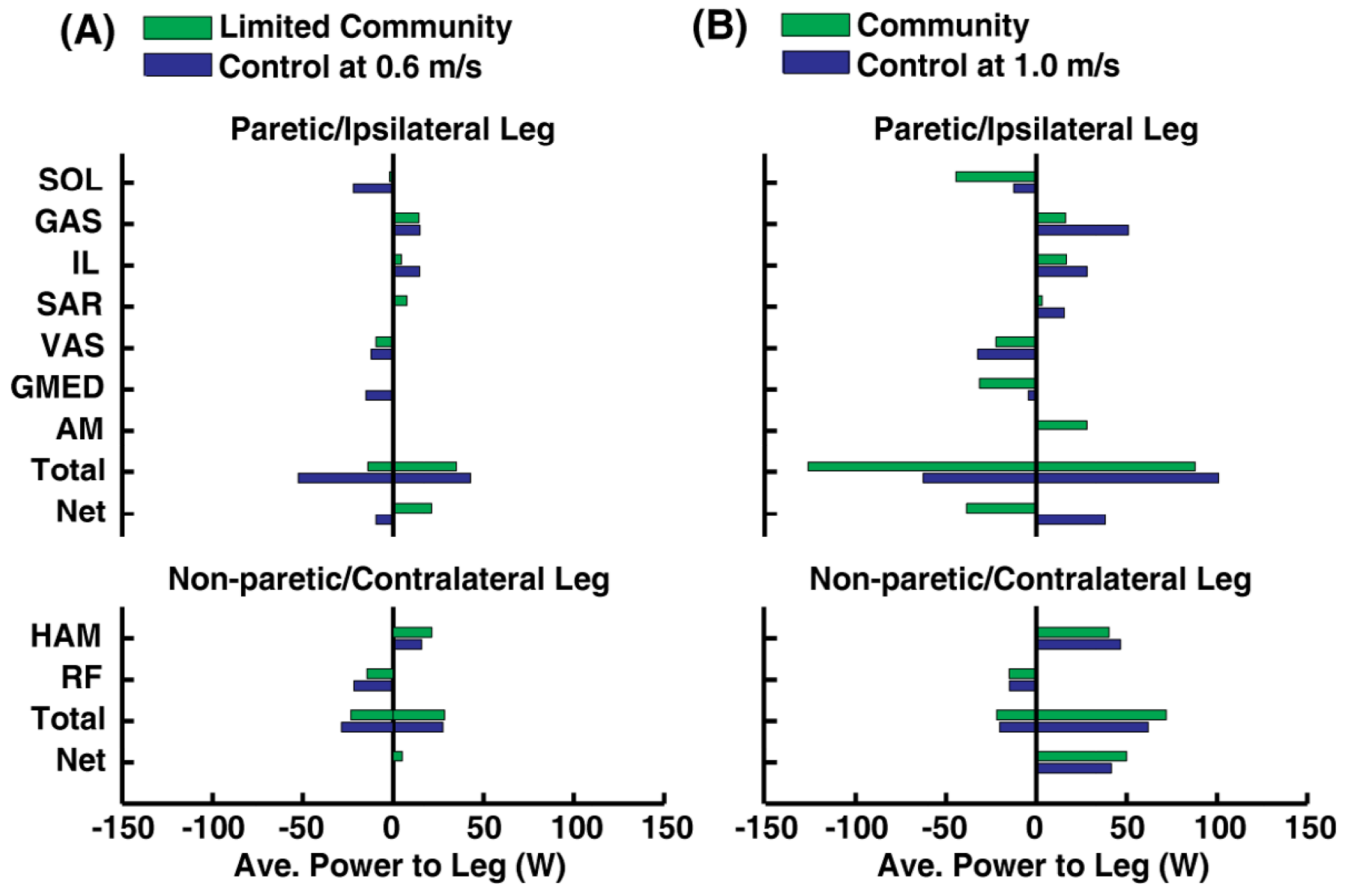


Fig. 4. Primary muscle contributors to average swing initiation during pre-swing by paretic (ipsilateral for control) and non-paretic (contralateral for control) leg muscles. (A) For the limited community walker, swing initiation by paretic muscles was similar to the ipsilateral control leg, but paretic muscles absorbed less power compared to the control. (B) For the community walker, swing initiation by the paretic GAS, IL and SAR was decreased and paretic AM was increased compared to the control. Paretic muscles absorbed much more power from the paretic leg compared to the ipsilateral control leg.

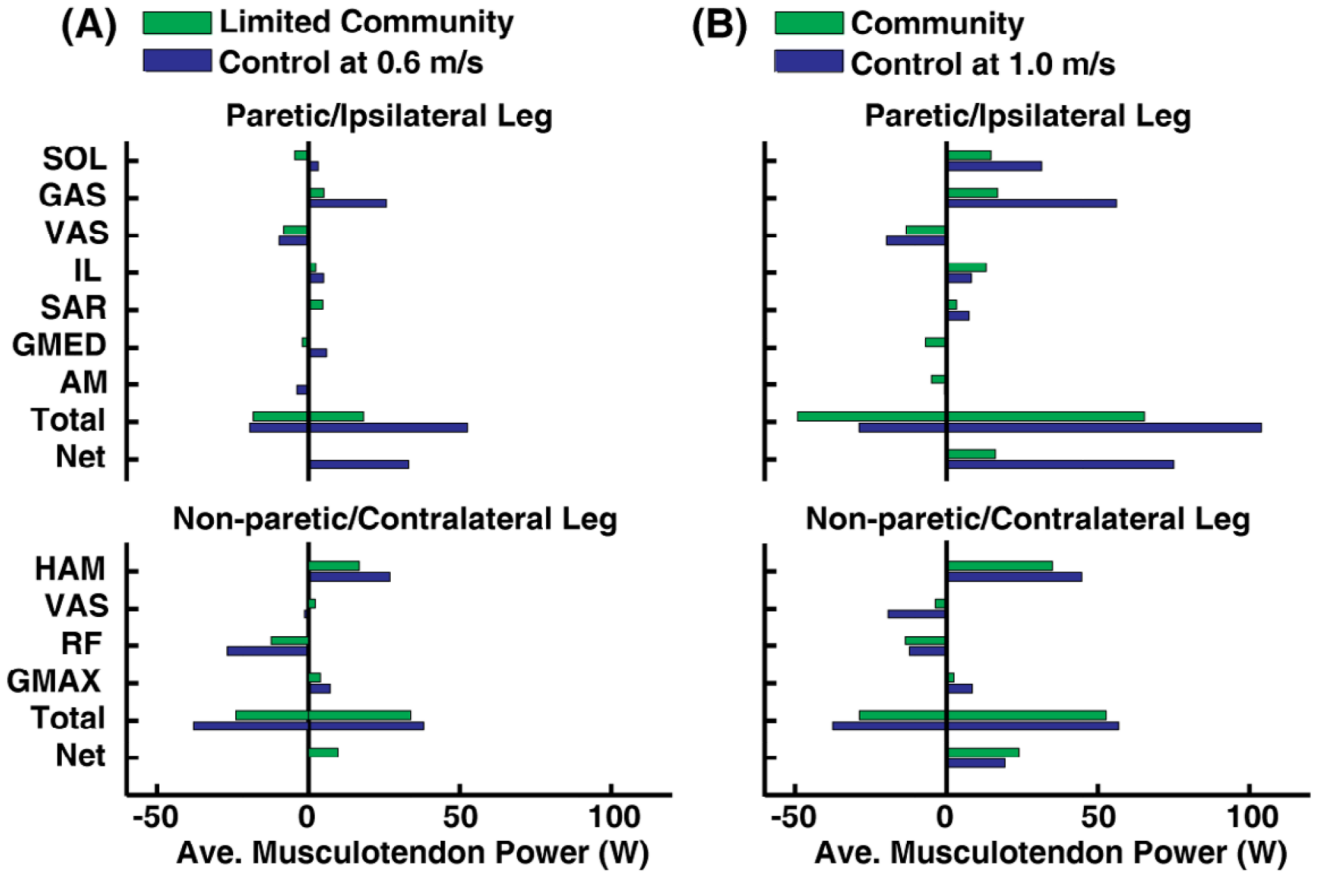


Fig. 5. Average power generated by paretic (ipsilateral for control) and non-paretic (contralateral for control) leg muscles during pre-swing. (A) Paretic muscles generated less power in the limited community walker relative to the speed-matched control as paretic GAS generated much less power. (B) The community walker generated and absorbed much power with the paretic and non-paretic leg muscles, although power generated by the paretic SOL and GAS was decreased relative to the control.

Table 1

The 43 musculotendon actuators per leg were combined into 18 groups after analysis according to their anatomical classification and contributions to the walking subtasks.

Muscle name	Analysis Group
Iliacus, Psoas	IL
Adductor Longus, Adductor Brevus, Pectineus	AL
Quadratis Femoris	QF
Superior, Middle and Inferior Adductor Magnus	AM
Sartorius	SAR
Rectus Femoris	RF
Vastus Medialis, Lateralis, and Intermedialis	VAS
Anterior, Middle and Posterior Gluteus Medius	GMED
Piriformis	PIRI
Gemellus	GEM
Anterior, Middle and Posterior Gluteus Minimus	GMIN
Tensor Fascia Lata	TFL
Anterior, Middle, and Posterior Gluteus Maximus	GMAX
Semitendinosus, Semimembranosus, Gracilis, Biceps Femoris Long Head	HAM
Biceps Femoris Short Head	BFSH
Medial and Lateral Gastrocnemius	GAS
Soleus, Tibialis Posterior, Peroneus Brevis, Flexor Digitorum Longus, Flexor Hallucis Longus	SOL
Tibialis Anterior, Extensor Digitorum Longus, Peroneus Tertius, Extensor Hallucis Longus	TA

Table 2

The average error between the experimental and simulated kinematics and ground reaction forces (GRFs) compared to the average standard deviations of the experimental data (in parentheses above).

	Limited Community	Control at 0.6 m/s	Community	Control at 1.0 m/s
Pelvis				
Obliquity	1.623 (2.193)	0.580 (1.150)	0.298 (1.364)	1.083 (1.207)
Rotation	1.249 (4.967)	2.532 (2.457)	1.775 (3.223)	0.570 (2.657)
Tilt	1.635 (2.946)	0.420 (1.481)	0.492 (1.893)	0.467 (1.442)
Trunk				
Obliquity	2.118 (2.154)	0.848 (1.540)	5.162 (3.178)	0.962 (1.364)
Rotation	1.236 (1.544)	0.671 (0.463)	1.776 (2.131)	0.272 (0.520)
Tilt	1.830 (1.605)	2.343 (1.240)	4.852 (1.445)	1.126 (2.130)
Ipsilateral/ Paretic Leg				
Hip Adduction Hip	1.020 (2.370)	2.731 (1.886)	1.435 (2.366)	3.660 (1.634)
Rotation	2.441 (4.568)	0.715 (2.532)	2.922 (5.058)	0.846 (2.170)
Hip Flexion	2.100 (6.227)	1.706 (3.905)	0.752 (3.911)	1.379 (3.347)
Knee Flexion	8.319 (9.909)	1.629 (5.059)	2.808 (6.409)	2.802 (4.012)
Ankle				
Dorsiflexion	3.783 (2.565)	0.643 (1.775)	1.108 (2.159)	1.889 (1.866)
Contralateral/ Non-Paretic Leg				
Hip Adduction	1.399 (2.575)	1.156 (1.955)	0.293 (1.853)	1.701 (1.911)
Hip Rotation	3.123 (4.296)	0.533 (3.272)	0.815 (4.732)	1.344 (2.659)
Hip Flexion	3.380 (5.264)	1.159 (2.617)	0.552 (3.230)	1.341 (2.612)
Knee	3.892 (7.138)	3.741 (6.434)	3.403 (6.163)	1.804 (5.120)
Ankle				
Dorsiflexion	1.286 (1.989)	0.457 (1.239)	0.491 (1.850)	0.646 (1.148)
Ipsilateral/ Paretic Leg				
A/P GRF	0.264 (0.620) 7.324	0.646 (2.111)	0.533 (2.689)	2.675 (2.450)
Vertical GRF	(11.365)	2.327 (7.479)	6.031 (14.027)	6.983 (11.959)
M/L GRF	3.024 (1.311)	1.834 (0.938)	1.133 (1.248)	3.019 (1.540)
Contralateral/ Non-Paretic Leg				
A/P GRF	0.655 (2.455)	1.368 (1.997)	0.505 (2.394)	1.174 (2.585)
Vertical GRF	8.365 (12.697)	3.975 (7.721)	4.181 (13.522)	6.391 (10.426)
M/L GRF	2.192 (1.632)	1.579 (1.103)	0.665 (1.563)	2.414 (1.997)
Forces(%BW)				
Average Angle Error (degrees)	2.527	1.367	1.808	1.368
Average GRF Error (%BW)	3.637	1.955	2.175	3.776